Sensors & Transducers

Design of an Electric Commutated Frog-Leg Winding Permanent-Magnet DC Machine

Hang Zhang, Yue-Jin Zhang, Chen Li, J. Z. Jiang

Department of Automation, Shanghai University, Shanghai, 200072, China
Tel.: (86)-021-56331266, fax: (86)-021-56331266
E-mail: zhanghang@shu.edu.cn

Abstract: An electric commutated frog-leg winding permanent-magnet (PM) DC machine is proposed in this paper. It has a semi-closed slotted stator with a classical type of mesh winding introduced from the conventional brushed DC machine and a polyphase electric commutation besides a PM excitation rotor and a circular arrayed Hall position sensor. Under the cooperation between the position sensor and the electric commutation, the proposed machine is basically operated on the same principle of the brushed one. Because of its simplex frog-leg winding, the combination between poles and slots is designed as 4/22, and the number of phases is set as 11. By applying an exact analytical method, which is verified comparable with the finite element analyses (FEA), to the prediction of its instantaneous magnetic field, electromotive force (EMF), cogging torque and output torque, it is well designed with a series of parameters in dimension aiming at the lowest cogging torque. A 230 W, 4-pole, and 22-slot new machine is prototyped and tested to verify the analysis. *Copyright © 2014 IFSA Publishing, S. L.*

Keywords: DC machine, Electric commutation, Permanent magnet, Simplex frog-leg winding.

1. Introduction

There is a long time for the seeking of non-contact commutated DC machine as early as 1934, owing to the fundamental weaknesses of a conventional brushed DC machine such as mechanical brushes and commutation spark which lead to many disadvantages like complex structure, difficult maintenance and restricted environment for practical use. Several researchers attempted to design a thyratron machine [1] using electronic tubes under the poor technical and economic conditions at that time, in which case the thyratron machine had been hardly evolved. Until 1960s, the striving for commutatorless DC machine has made great progress since the appearance of thyristors (SCRs), prompting the realization of commutatorless machine (CLM) [2]. A CLM is generally such a system in combination of a synchronous motor having a three-phase star-delta winding and a three-phase thyristor inverter which supplies synchronous AC power corresponding to the rotating frequency. From then on, more and more worldwide researchers focused on the electric commutation, and then the research direction was evolved into two branches, i.e., AC and quasi-DC electric commutation. In late 1970s, Yukio Takeda and Kenya Sakamoto from Japan, on behalf of the quasi-DC electric commutated machine branch, proposed a thyristor brush machine (TBM), which is composed of a polyphase drum type closed coil armature and a polyphase thyristor bridge rectifier (i.e. converter) circuit, as equivalent DC machine, and it has fundamentally the same characteristics as that of the conventional DC

machine [3]-[5]. However, the most published papers focus on the AC electric commutated (i.e. inverter) machine, which evolved into the well-known brushless DC machine (BLDC). The transient of TBM indicates the bottlenecks in power switching device development at that time on one hand, and the significant development of BLDC on the other hand, therefore, it vanished from most people's sight for nearly half a century.

Considering the output torque and power of BLDC will be limited by the existence of internal inductance as it would cause worse mechanical characteristics than that of a brushed DC machine near the breakdown torque, and it is more difficult to realize speed range extension [6]-[13], a new DC machine whose brushes and field winding is replaced by an electric commutation and PMs respectively is proposed. It seems that the evolution of commutator-less DC machine will be back to the TBM to point out a better solution, i.e., a new design and simulation method of TBM can reproduce its role in non-contact commutated DC machine and it still can be operated in the same way as a brushed one but not a BLDC nowadays.

Until 2009, the TBM attached people's attention again, mainly in China. A simplex wave winding PM brushless DC machine with a special combination number of pole and slot, i.e., 10-pole and 11-slot [14]-[15], is typically designed in several aspects, such as lower peak cogging torque thanks to the "goodness" factor of slot number and pole number combination [16] with the value of 1, less copper loss owing to the reduced winding pitch as 1, smaller volume for higher pole number as 10 and wider speed range on account of properly controlling the switch status to decrease the number of coils connected into the equivalent circuit. However, because of its simple simplex wave winding, it leaves fault tolerance out of consideration, and its analytical model, which is based on conformal mapping considering slotting effect, doesn't seem so accurate that the results from this analytical model are not compatible with that of corresponding FEA at the positions of air-gap under slot. With the same theory, a new 4-pole and 18-slot simplex lap winding PM brushless DC machine has been put into practice for the application requiring high speed no less than 10,000 rpm, such as direct-driven twister [17]. According to the split number of phases of armature coil of this motor as 9, the total number of power electronic switching devices adopted in the electric commutation is 18, which is less than that of the 10-pole/11-slot machine as 22. Nevertheless, most of their work focus on the operation of this new DC machine, such as sensorless control scheme and circuit analysis of armature [18]-[21], rather than its electromagnetic field calculation and analysis for machine ontology design. Moreover, they have made two low-level misunderstandings in the inverse of control (IOC) by just inversing current flowing through coils without any consideration of Hall arrangement, and the choice of armature winding for high-speed application. Consequently,

there are several issues need to be improved, for instance, the simplex lap winding with winding pitch as 4 means longer end of coil resulting in more copper loss, the equalizer should be configured for the simplex lap winding to ensure stable operation, and it takes no account of fault-tolerance either.

As always there is a trade-off, in order to be applied to direct drive applications featuring higher torque at low speed, wide speed range and fault-tolerance, passing over the copper loss and processing difficulty, the new DC machine dealt with in this paper, is such a electromechanical system formed by a PM synchronous motor having a frog-leg armature as a stator, and a polyphase electric commutation having the same number of phases equals to the split number of phases of armature coil of the motor as 11. By properly controlling the 11-phase electric commutation according to the exact energizing sequence in a given revolving direction of the rotor, its operation principle is basically the same as a brushed one, whereby it not only keeps the characteristics of a brushed DC machine such as wide operating speed range, smooth speed regulation, overload capacity and high holding torque, but also improves the efficiency and power density. Both the theoretical analysis and experimental results validate the feasibility of the proposed electric commutated frog-leg winding PM DC machine.

2. Machine Structure Characteristics

The proposed machine is not really a new invention as a whole for it combines an inverted conventional DC machine and a polyphase electric commutation composed of 11 electric commutator segments, i.e., 11 half-bridges, every of which is assembled by 2 power switches, and then the control logic and energizing sequence of power electronic switches substitutes for the relative motion between mechanical commutator and carbon brush. As summarized foregoing from a perspective based on the operation of the proposed DC machine, it turns to the topic of machine design as if it is a combination of a PM synchronous DC machine with a frog-leg armature and an 11-phase quasi-DC electric commutation, from which it attributes the success to the design of frog-leg armature inherited from the conventional brushed DC machine.

It is essential to concern the commutation process in the design of a DC machine in general. To ease the commutation process and ensure stable operation, the branch potential and current distribution in the winding should be balanced, which would be destabilized by many unforeseen reasons leading to uneven magnetic reluctance or air gap, such as discontinuity of material, installation error and deformation of shaft. Therefore, the equalizer has always been configured for the conventional DC armature winding to avoid this case. As referred to the simplex lap winding without equalizer, the coils from the same branch are placed under the different

magnetic poles, if the magnetic reluctance or air gap is nonuniform, then there would be unbalanced branch potential caused by unequal magnetic flux under magnetic poles. Moreover, a surge circulation current would be generated by a little disturbance in potential and smaller internal resistance of armature winding. At last, when it operates on load, the distribution of current between the two branches becomes seriously imbalanced, which leads to overheated armature with more copper loss. However, there is no need to install equalizer for the simplex wave winding for its connection principle is just the same as a natural equalizer.

Although the configured equalizer can reduce copper loss and improve commutation, it makes the armature more complicated and wastes more copper. Therefore, a simplex frog-leg winding is introduced, for the same purpose as the equalizer to make full use of the copper, to be employed in the proposed DC machine because of its excellent potential for use under high voltage and large current to obtain wide speed range and high torque besides fault tolerance.

The rules for designing a simplex frog-leg winding of DC machines are presented below [22],

$$\begin{cases} m = p \\ y_{1L} + y_{1W} = K/p \\ y_{kL} + y_{kW} = K/p \ , \\ y_{kL} = \pm 1 \\ y_{1L} = K/2p \pm \varepsilon \end{cases} \quad (1)$$

where p is the number of pairs of poles, m is the degree of multiplicity of the wave winding, that is, m=1 for simplex wave, 2 for duplex, and so forth, K is the number of slots, which is the same as that of commutator bars of a conventional DC machine, y_{1L} and y_{1W} is the winding pitch of the lap winding and wave winding respectively, y_{kL} and y_{kW} is the virtual commutator pitch of the lap winding and wave winding respectively, ε is a correction to make y_{1L} an integer.

It ought to take the electric commutation in consideration for the armature winding design of the proposed machine, because the torque ripple arose from the jumping magnetomotive force (MMF) decreases as the number of edges of the closed winding, which equals to that of the phases of electric commutation is increased. There is a trade-off between the number of power electronic switches and the amplitude of torque ripple, and then the mean number of series coils per path N_{2a} is set as 5.5 which is same with [14]. Besides, the simplex frog-leg armature winding with the degree of multiplicity of the wave winding is set as m=2 in common use. Therefore, according to formula (1), the number of poles is 2p=4 and the total number of pairs of parallel paths is a=a_L+a_W=4, that is, the number of pairs of parallel paths through the simplex lap winding a_L is equal to p as 2 and that of the duplex wave winding a_W is equal to m as 2, and then the total number of coils is N=44 by multiplying N_{2a} and $2a$. From the above, it comes to a conclusion that the number of slots is K=22 for there are 2 complete windings on the armature to average N. Since the coils' ends connected to the virtual commutators cross each other leading to more copper waste as y_{kL}=-1 and y_{kW}=11, when y_{kL}=1 and y_{kW}=10, either y_{1L}=5 and y_{1W}=6, or y_{1L}=6 and y_{1W}=5 is obtained. In conclusion, the proposed machine is designed with 4 poles and 22 slots, and it has a simplex frog-leg armature winding of simplex lap and duplex wave with the number of winding/virtual commutator pitch as y_{1L}=5/y_{kL}=1 and y_{1W}=6/ y_{kw}=10 respectively.

From the given parameters calculated above, the developed winding diagram of a simplex frog-leg armature winding with 4 poles and 22 slots including 22 commutator bars and 4 carbon brushes can be drawn according to its drawing principle. It is obvious that the 4 fixed symmetrical brushes divide the armature winding circuit into 2 paralleling units. Inspired from this, a novel 11 split phases armature winding for the electric commutated PM DC machine emerges, i.e. Fig. 1.
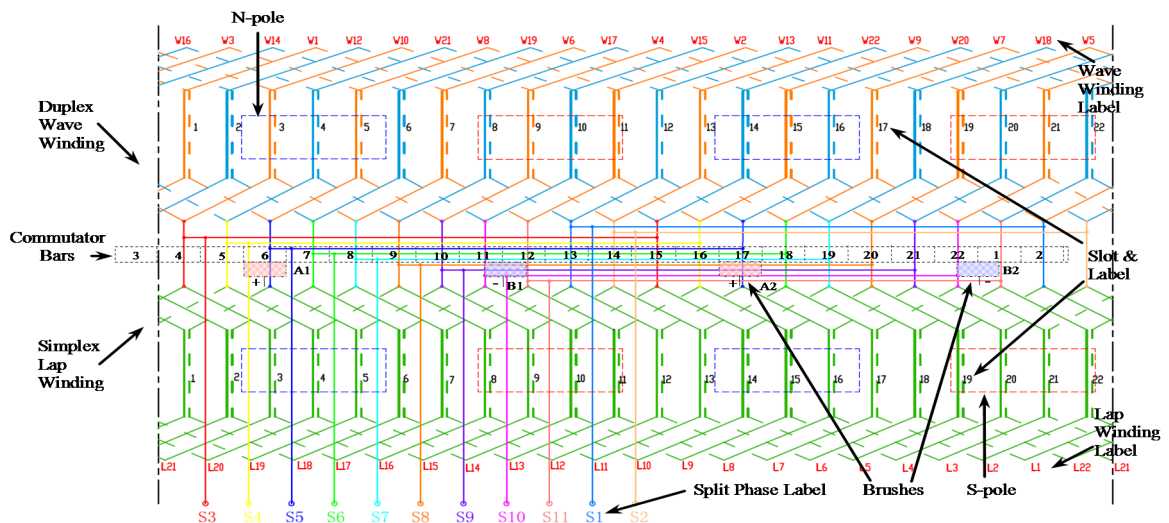

Fig. 1. Simplex frog-leg armature winding.

Eliminating the 22 commutator bars and 4 carbon brushes of the conventional DC machine with simplex frog-leg armature winding, and connecting every two coils' ends contacted to the same pole of brushes together by assuming that the brushes are forwarding in a certain direction, a special armature winding type is presented for the electric commutated PM DC machine, with the split number of phases of armature coil as 11, which is illustrated in Fig. 1. Although it is indeed more complex than either of the new DC machines referred in section 1, the final commutation circuit is unexpectedly symmetrical like a spider web named araneose coil armature and even more advanced as shown in Fig. 2.
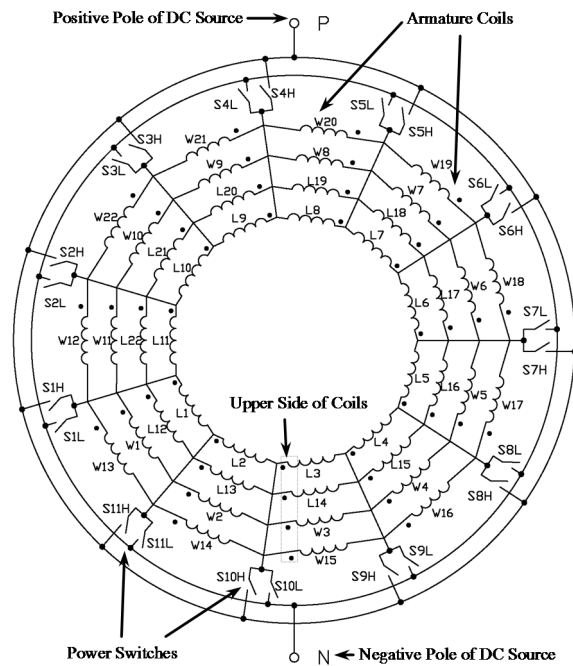
Fig. 2. Commutation circuit.

Compared to the commutation circuits of the two new DC machines, each coil of the original commutation circuit is replaced by 4 coils connected in parallel, which means larger armature current arose from smaller resistance of armature winding under the same voltage and better fault-tolerance.

Taken away the armature winding, what it gets is just the rotor and stator of a BLDC machine with surface-mounted PMs as shown in Fig. 3. The dimensions are well-designed using an analytical method, which will be introduced in section 4, based on the analysis of electromagnetic field which is more accurate and fast, while neither magnetic circuit method nor FEA method has yet met the goals of both accuracy and rapidity. In addition, paying attention to the 4 layers along the height of slot for the two complete double-layer windings on the armature, the wave winding should be placed on the first and forth layers from above down, while the lap winding should be placed on the second and third layers accordingly.
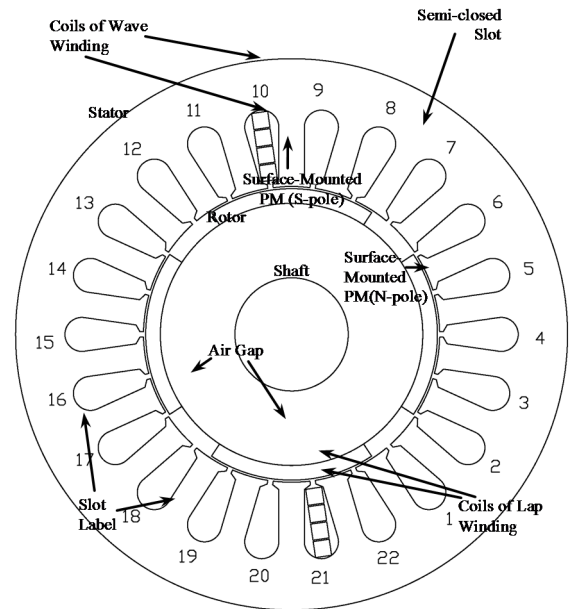

Fig. 3. 2-D view of stator and rotor.

3. Principle of Operation

The operation principle of the proposed machine is basically as same as a brushed DC machine that in brief the current direction of coils under N or S pole remains unchanged by accurately controlling the power electronic switch status [14]. However, it is only the presentational rules concluded from the operation of a brushed DC machine, instead of the fundamental principle to rotate it which demonstrates the essential difference between the proposed machine and the well-known machine (BLDC) that the rotational magnetic field is generated by quasi-DC rather than AC.

It is not an exclusive physical phenomenon of a three-phase symmetry AC armature energized by three-phase symmetry AC to generate a circular rotating magnetic field, which is regarded as an important basis in the operation analysis of AC synchronous or asynchronous machines. The quasi-DC armature, as shown in Fig.2, energized by a specific form of quasi-DC, which is generated by properly controlling the 11-phase electric commutation according to the exact energizing sequence in counterclockwise direction of the rotor as shown in Table 1, could also generate a rotating magnetic field.
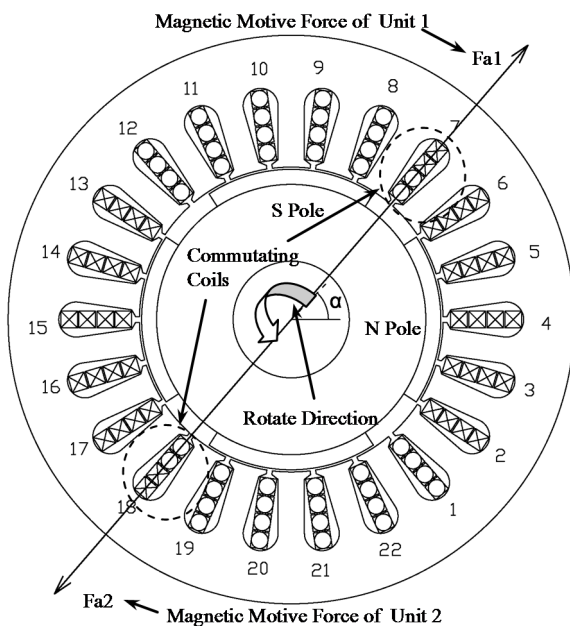
From Fig. 2, the number of the two current direction paths is not the same, that is, the number of coils under a pair of poles is odd as 11, which is convenient for the control of the 11-phase electric commutation as it only needs to change one switch from one status to another, as shown in Table 1. Therefore, assuming the DC bus current amplitude is I_d, then the phase current of every four layers after commutation fluctuates between $I_d \times 5/11$ and $I_d \times 6/11$ for each commutation in other phases. The wave form of phase current is roughly shown in Fig. 4.

**Table 1.** Energizing sequence of power electronic switch.

P		7	8	9	10	11	1	2	3	4	5	6	
N	1	2	3	4	5	6	7	8	9	10	11	1	
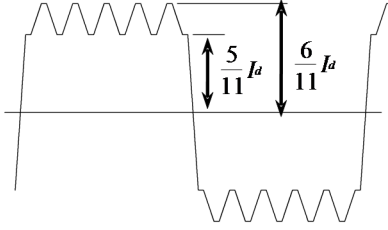
Fig. 4. Wave form of phase current.

When *S6H* and *S1L* are turned on as the first status in Table 1, coil *L7*, *L8*, *L9*, *L10*, *L11*, *L18*, *L19*, *L20*, *L21*, *L22*, *W7*, *W8*, *W9*, *W10*, *W11*, *W19*, *W20*, *W21*, *W22*, and *W12*, with the total number as 20 (5 coils per path), have the same current direction, and so for coil *L6*, *L5*, *L4*, *L3*, *L2*, *L1*, *L17*, *L16*, *L15*, *L14*, *L13*, *L12*, *W6*, *W5*, *W4*, *W3*, *W2*, *W1*, *W18*, *W17*, *W16*, *W15*, *W14*, and *W13*, with the total number as 24 (6 coils per path). Therefore, the current direction of each layer of slot with *S6H* and *S1L* on at α = 0 can be exhibited in Fig.5, where the circle in slot means the current direction is vertical out of the paper, and the cross in slot means the opposite current direction. While from another point of view, i.e., when and which switches to be turned on to supply a quasi-DC to drive the machine to rotate counterclockwise, since there are 2 units, it can be electrically equivalent to a 2-pole machine, and the upper side coils' position can be rearranged according to their original position under N or S pole as shown in Fig. 6.

From Fig. 5 (b), if we want the machine to rotate counterclockwise, coils under the same pole should have the same current direction with the right hand rule to orient the MMF keeping 90 electrical degree with PM MMF in advance, and then it gets the same current distribution referred in the previous paragraph. Pay attention to slot 7 and 18, the resultant current is zero, which means coil *L1*, *L12*, *W1* and *W13* are commutating.
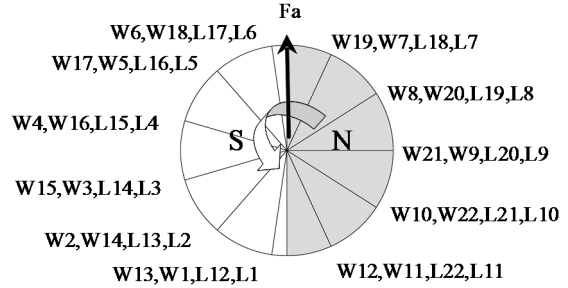
Fig. 6. Coils' position under 2-pole (α =0).

Besides the switch status (*S6H*, *S1L*), the other switch statuses can also generate an effective MMF through the 11-phase electric commutation as long as the distance between the two switches is the same as the pitch of pole, and then all the effective switch statuses can be deduced by rotating the 2-pole rotor counterclockwise every α = (2π/p)/22 = π/22 to determine the coils' current direction and the switches to be turned on. The total number of effective switch statuses is 22, as listed in Table 1. As a consequence, the current distribution along the armature surface is just a symmetrical square waveform, the space period of which is a pair of poles, as shown in Fig. 7.

Fig. 5. Current of coils (*S6H* and *S1L* on at α=0).
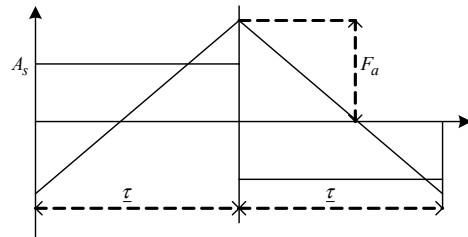
Fig. 7. Distribution of current along armature surface.

In Fig. 7, it assumes that the energized coils concentrated in slots are equivalent to a current sheet distributed along the circumferential surface of armature hence MMF of armature F_a generated by the current sheet is a triangle wave [23], whose amplitude can be obtained by

$$F_a = As\tau/2, \tag{1}$$

$$A_S = N_1 I_{a1}/t \tag{2}$$

$$\tau = \pi D/2p, \tag{3}$$

where A_S is the line load along the armature surface, N_l is the number of coils' sides in each slot, I_{al} is the current of each path, t is the pitch of teeth, D is the diameter of armature, and $\underline{\tau}$ is the pitch of pole.

The position of MMF peak at the interface of positive and negative current is just the space position of axis of MMF indicated by F_a as shown in Fig. 5, from which it can be concluded that the switch status should be renewed for certain coils' commutation at every $\pi/22$ mechanical position angle of rotor to generate an effective MMF to keep the rotor rotating in a certain direction. Therefore, according to the switch status sequence in Table 1, the MMF generated by quasi-DC is rotating counterclockwise with the aid of the 11-phase quasi-DC electric commutation. As a result, the rotor with surface-mounted PMs follows. Finally, as a quasi-DC machine, its rotation speed can be conveniently regulated by controlling the DC bus voltage or the switch statuses to update the number of coils connected into the equivalent circuit [14].

4. Simulation and Experiments

As referred in section 2, an exact analytical method, which is based on the solutions of Laplace's and Possion's equations using magnetic vector potential for air-gap, PM and slot domains under boundary and interface conditions [24], for predicting the instantaneous magnetic field, EMF induced in the armature winding, cogging torque and output torque of the proposed DC machine [25], is comprehensively introduced to provide an accurate and fast scheme for well-designed dimensions compared to FEA. It aims at lower peak cogging torque and higher torque density for the proposed machine.

For the sake of convenience and generality of the introduced exact analytical method, the detailed solutions for the model are omitted. In Fig. 8, the comparisons between analytical method and FEA are illustrated, and they are compatible with each others while the analytical method costs less time to predict the performance of the new machines with different dimensions, which means an efficient and effective way to design a new DC machine.

Table 2. Major Parameters.

Rated Power	230 W
Rated Voltage	48 V
Rated Speed	220 rpm
Rated Load	10.5 Nm
Pole/Slot Number	4/22
Stator Outer Diameter	151 mm
Stator Inner Diameter	81 mm
Stator Axial Length	101 mm
Thickness of Magnets	4 mm
Mechanical Air Gap	0.6 mm
Magnet Remanence	1.15 T
Slot Open Width	1.5 mm
Pole Arc Coefficient	0.74

(a) No-load field distribution.

(b) Back-EMF (Phase W1 at 220 rpm).

(c) Armature reaction field distribution.

(d) Magnetic field distribution on load.

(e) Electromagnetic torque.
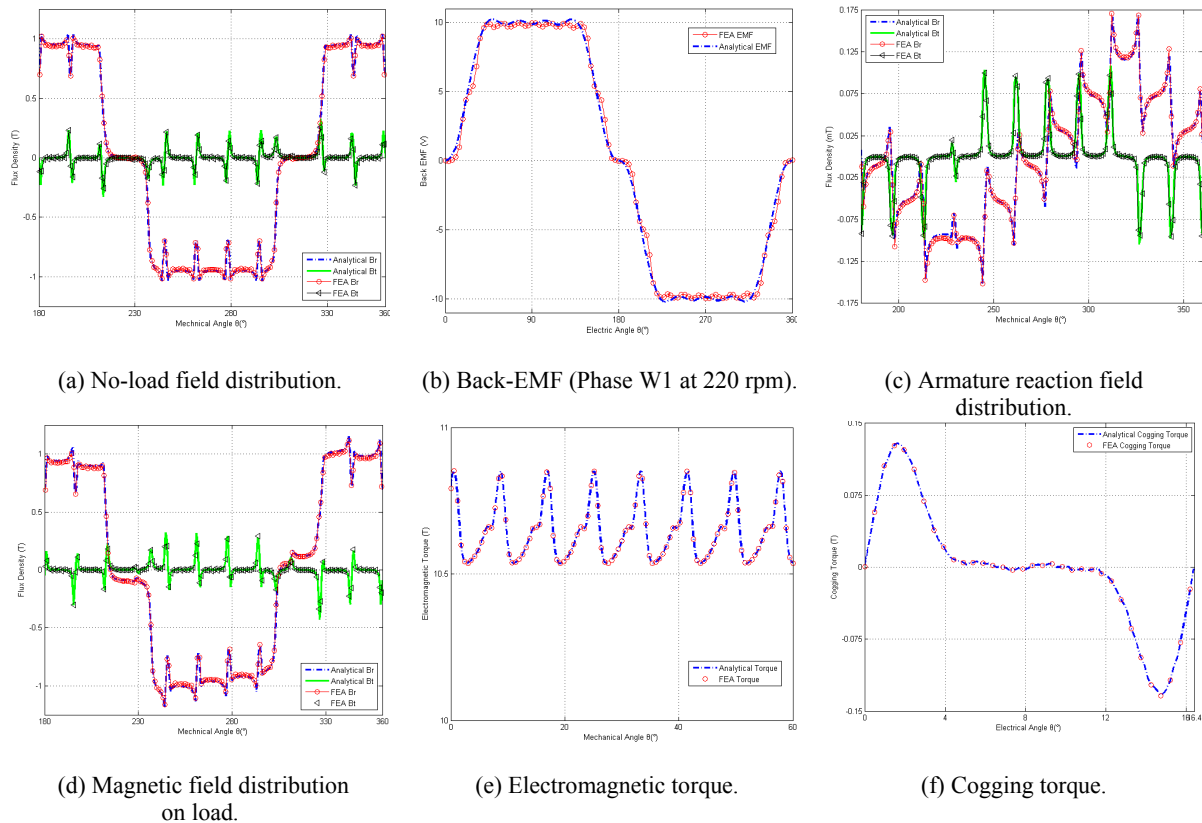

(f) Cogging torque.

Fig. 8. Simulation comparisons.

Its major parameters can be determined by the rated value and the repeated calculation of peak cogging torque from the exact analytical model to make it lower, i.e., adjusting the slot open width considering manufacturing process and pole arc coefficient based on the predicted optimal effective pole arc coefficient [26], as given in Table 2. Its general assembly drawing is illustrated in Fig. 9.
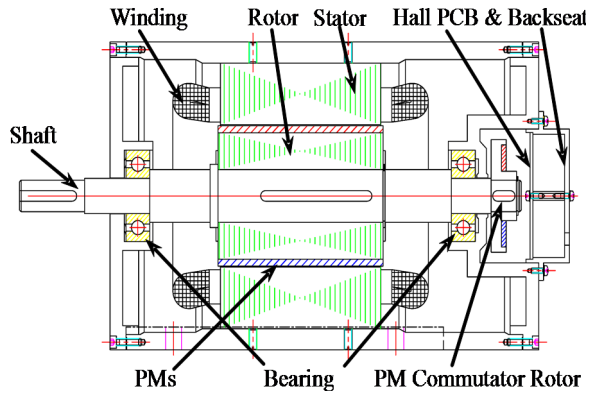

Fig. 9. General assembly drawing of prototype.

From Fig. 8(c), the maximum calculated cogging torque is 0.13 Nm while the electromagnetic torque is about 10.5 Nm, and then the predicted torque ripple caused by cogging torque is lower than 2 %. Since there are 11 phases of the armature winding, considering the axial magnetic field of specially designed PM commutated rotor, the position sensor should be accurately equipped with 11 Hall elements arrayed evenly around the center hole on the PCB board as shown in Fig. 10(c). To validate the principle of proposed DC machine and the simulation model, the prototype is used as a generator driven by a conventional DC machine as shown in Fig. 10(a), and the no-load EMF wave forms of phase 1 and phase 2 at the speed of 110 rpm are recorded using an oscilloscope and then compared with corresponding simulation results, as shown in Fig. 11. We can learn that the maximum no-load EMF is about 5 V at the speed of 110 rpm.

Observing Fig. 8 (b) and Fig. 11, we can find that there are distinct differences between the no-load EMF wave forms of analytical and FEA, while that of experiment is basically the same with FEA, on the hillside between zero and the positive or negative maximum EMF. It is likely due to the assumption for the modeling of analytical method that the gaps between poles are filled with a kind of virtual material with the same permeability of PMs, which leads to smooth magnetic flux under pole. Beyond that, results from experiment are still compatible with corresponding simulation, and the design of the proposed DC machine is validated.
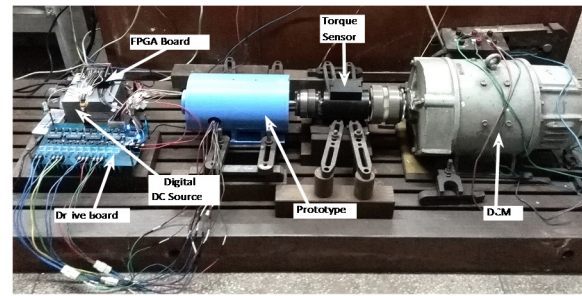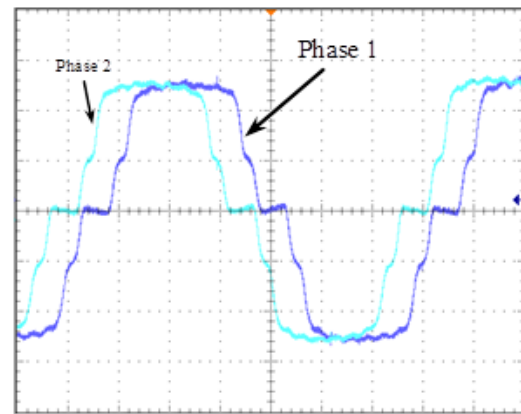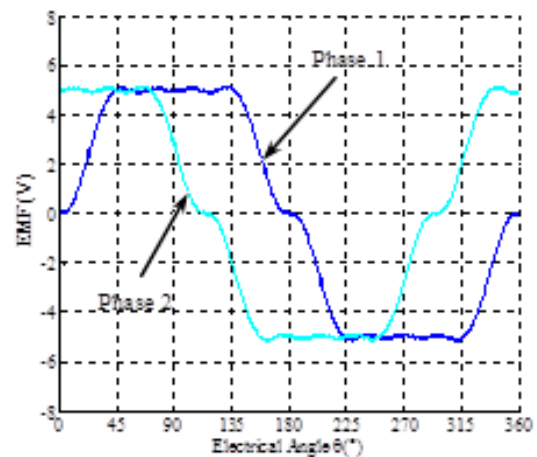

(a) Experimental platform.
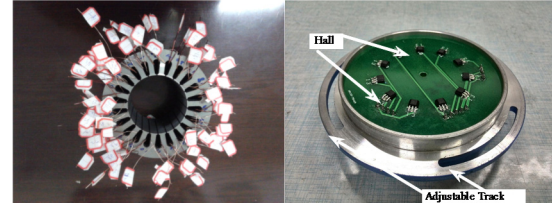
(b) Wiring stator.   (c) Adjustable Hall PCB backseat.

Fig. 10. Prototype components and experimental platform.

(a) Experimental results. (2 V/div, 40 ms/div, 110 rpm)

(b) Simulation results (110 rpm).

Fig. 11. No-load EMF wave forms of phase1 and phase 2.

5. Conclusions

An electric commutated frog-leg winding PM DC machine has been proposed, and experiments are carried out. The new DC machine is regarded as a system in combination of a PM synchronous machine having a frog-leg armature as a stator, and an 11-phase electric commutation besides an 11-phase circular arrayed Hall position sensor. By properly controlling the electric commutation according to the exact energizing sequence, the operation principle of this new DC machine is basically the same as a brushed one, whereby it not only keeps the characteristics of a brushed DC machine, but also improves the efficiency and power density. Finally, the results comparison between the simulation, based on the proposed exact analytical method and FEA, and the prototype experiments validate the feasibility of the design proposal.

Compared to the two machines with the same theory referred in section 1, it contributes the novelty of the proposed new DC machine to the design of frog-leg armature inherited from the conventional brushed DC machine. Besides, a more efficient and effective method to design a new DC machine based on a general exact analytical model turns out to be a novel way to rival FEA method, and the quasi-DC armature winding could also be promoted to whether asynchronous or synchronous machines for the future work.

Acknowledgments

References

[1]. E. F. W. Alexanderson, A. H. Mittag, The thyratron motor, *Electrical Engineering*, Vol. 53, 1934, pp. 1517-1523.

[2]. O. Eiichi, K. Takeshi, and A. Masahiko, The thyristor commutatorless motor, *IEEE Transactions on Magnetics*, Vol. 3, Issue 3, 1967, pp. 236-240.

[3]. T. Yukio, S. Kenya, and M. Iwao, On the thyristor brush motor, *Conference Record of Spring Lecture Meeting of MESJ*, 1976, No. 114 (in Japanese).

[4]. T. Yukio, et al., On the thyristor brush type dc machine, *Bulletin of MESJ*, Vol. 5, No. 2, 1977, pp. 177-184.

[5]. T. Yukio, et al., On the generator characteristics of the thyristor brush type dc machine, *Bulletin of MESJ*, Vol. 6, No. 1, 1978, pp. 61-68.

[6]. T. M. Jahns, Flux-weakening regime operation of an interior permanent-magnet synchronous motor drive, *IEEE Transactions on Industry Applications*, Vol. IA-23, No. 4, 1987, pp. 681-689.

[7]. W. Soong, T. J. E. Miller, Field-weakening performance of brushless synchronous ac motor drive, *IEEE Transactions on Industry Applications*, Vol. 141, No. 6, 1994, pp. 331-340.

[8]. A. Fratta, A. Vagati, and F. Villata, Design criteria of an IPM machine suitable for field-weakened operation, in *Proceedings of the ICEM.*, Sep. 1990, pp. 1059-1064.

[9]. M. Barcaro, N. Bianchi, and F. Magnussen, Design considerations to maximize performance of an IPM motor for a wide flux-weakening region, in *Proceedings of the XIX ICEM*, 6-8 Sep. 2010, pp. 1-7.

[10]. D. G. Dorrell, M. Hsieh, et al., A review of the design issues and techniques for radial-flux brushless surface and internal rare-earth permanent-magnet motors, *IEEE Transactions on Industrial Electronics*, Vol. 58, No. 9, 2011, pp. 3741-3757.

[11]. T. M. Jahns, Torque production in permanent-magnet synchronous motor drives with rectangular current excitation, *IEEE Transactions on Industry Applications*, Vol. IA-20, No. 4, 1984, pp. 803-812.

[12]. J. F. Gieras and M. Wing, Permanent magnet motor technology: design and applications, *Marcel Dekker*, New York, 2002.

[13]. S. Chaithongsuk, B. N. Mobarakeh, et al., Optimal design of permanent magnet motors to improve field weakening performances in variable speed drives, *IEEE Transactions on Industrial Electronics*, Vol. 59, No. 6, 2012, pp. 2484-2494.

[14]. L. Zhu, S. Z. Jiang, J. Z. Jiang, et al., A new simplex wave winding permanent-magnet brushless DC machine, *IEEE Transactions on Magnetics,* Vol. 47, No. 1, 2011, pp. 252-259.

[15]. L. Zhu, S. Z. Jiang, J. Z. Jiang, et al., Speed range extension for simplex wave winding permanent-magnet brushless DC machine, *IEEE Transactions on Magnetics*, Vol. 49, No. 2, 2013, pp. 890-897.

[16]. L. Zhu, S. Z. Jiang, Z. Q. Zhu, et al., Analytical methods for minimizing cogging torque in permanent-magnet machines, *IEEE Transactions on Magnetics*, Vol. 45, No. 4, 2009, pp. 2023-2031.

[17]. Z. P. Wang, M. X. Chen, M. Y. Xu, et al., Practice on the new generation of DC motor (New DCM), *Micromotors*, Vol. 43, No. 11, 2010, pp. 1-6 (in Chinese).

[19]. Z. P. Wang, M. X. Chen, About armature winding and armature circuit of DC motor circular current problem (Part 1), *Micromotors*, Vol. 45, No. 7, 2012, pp. 1-5 (in Chinese).

[20]. Z. P. Wang, M. X. Chen, About the armature winding and armature circuit of DC motor (Part 2) armature main circuit, *Micromotors*, Vol. 45, No. 9, 2012, pp. 6-12 (in Chinese).

[21]. M. X. Chen, L. Chen, and Z. P. Wang, Analysis of armature circuit of the new DCM, *Micromotors*, Vol. 46, No. 4, 2013, pp. 8-13 (in Chinese).

[22]. H. B. Dwight, R. G. Haltmaier, Rules for designing frog-leg windings of DC machine, *Transactions of the American Institute of Electrical Engineers*, Vol. 70, Issue. 1, 1951, pp. 707-712.

[23]. Z. P. Wang, M. X. Chen. New theory of DC motor, Micromotors, Vol. 45, No. 1, 2012, pp. 1-6 (in Chinese).

[24]. J. B. Li, L. B. Jing, et al., Exact analytical method for surface-mounted permanent-magnet brushless motors, *Transactions of China Electrotechnical Society*, Vol. 27, No. 11, 2012, pp. 83-88 (in Chinese).
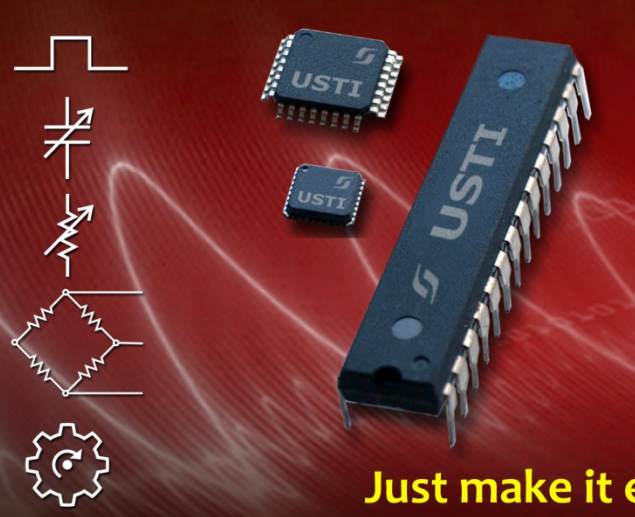
[25]. A. Bellara, Y. Amara, et al., Two-Dimensional exact analytical solution of armature reaction field in slotted surface mounted PM radial flux synchronous machines, *IEEE Transactions on Magnetics*, Vol. 45, No. 10, 2009, pp. 4534–4538.

[26]. L. Zhu, S. Z. Jiang, Z. Q. Zhu, et al., Analytical methods for minimizing cogging torque in permanent-magnet machines, *IEEE Transactions on Magnetics*, Vol. 45, No. 4, 2009, pp. 2023-2031.

———————————